Self-Interacting Gravity and the Transition from Radial to Transport-Dominated Gravitational Dynamics

Jorgen Karlsen

Abstract

The dynamics of galaxies present a long-standing challenge to gravitational theory. While Newtonian gravity and General Relativity describe solar-system phenomena with high precision, observed galactic rotation curves deviate systematically from the inverse-square expectation at large radii.

In this work, we explore an alternative approach in which gravitational influence is treated as a conserved outward transport that undergoes progressive redistribution through interaction with the vacuum. Modeling this redistribution as a stochastic scattering process using a Poisson description, leads to a closed-form analytical expression for the gravitational field,

$$g(r) = \frac{GM_b}{r^2} e^{-r/\lambda} + \frac{GM_b}{\lambda r},$$

which describes a continuous transition from a geometry-dominated inverse-square regime to a redistribution-dominated $1/r$ regime. When combined with the mass-dependent transport scale $\lambda = \sqrt{GM_b/a_0}$, this framework yields an asymptotic field $g(r) \sim \sqrt{GM_b a_0}/r$, consistent with the empirical baryonic Tully–Fisher relation. Furthermore, the emergence of an effective $1/r$ regime influences the dynamics of galactic cores, where distance-enhanced gravitational contributions lead to a breakdown of Newton's shell theorem and naturally produce stiff-core rotation.

Within this framework, galactic dynamics arise from transport behavior and statistical self-interaction, allowing a consistent description based solely on baryonic matter, without introducing additional matter components. The resulting force law applies across different galactic scales without parameter tuning, providing a predictive and testable description of observed galactic kinematics.

1. Introduction

General Relativity [1] and Newtonian gravity describe solar-system dynamics with extraordinary precision, while galactic rotation curves systematically deviate from the inverse-square expectation at large radii. Observations show that rotation curves of spiral galaxies remain approximately flat at large radii [2, 3], in contrast to the decline expected from the inverse-square law applied to the observed baryonic mass distribution.

The prevailing explanation introduces non-baryonic dark matter [4, 5] to provide additional gravitational influence. While successful phenomenologically, this approach relies on the existence of matter that has not been directly detected and whose distribution must be inferred indirectly. This has motivated alternative approaches, including phenomenological modifications of gravitational laws such as MOND [6]. While successful in certain scaling relations, such modifications often lack a clear dynamical mechanism for the transition between regimes.

An alternative approach is to reconsider how gravitational influence propagates through space. Rather than modifying the gravitational interaction or introducing additional matter, one may ask whether the observed behavior can arise from the dynamics of gravitational transport itself.

1.1 Gravity as a transport process

In the present work, gravity is treated as a continuous outward transport generated by baryonic sources and propagating through a vacuum medium. The key assumption is that the source (mass) has a constant output of gravity, while the redistribution process is independent of time. The directional coherence of the transport is progressively redistributed through elastic interactions with the vacuum. Since time is not an issue, the source keeps feeding an ever increasing volume of redistributed gravity with increasing distances from the source.

This redistribution does not change gravitational influence, but alters how it is carried and distributed in space. As transport is shared among an increasing number of carriers, the effective outward drift velocity decreases with distance.

A reduction in drift velocity leads to an increase in the local density of transported influence. This increase manifests as an enhancement of the gravitational field relative to the purely geometric inverse-square behavior.

1.2 Emergence of galactic-scale behavior

Importantly, this behavior arises from the dynamics of transport and vacuum self-interaction, rather than from an ad-hoc modification of inertia. By recognizing that the vacuum interacts with the statistical fluctuation of the field ($\sqrt{M}$) rather than its macroscopic baryonic intensity (M), the framework yields a single, unified force equation across all radii. In this picture, the transition scale is not imposed externally but emerges natively from the geometric threshold $\lambda = \sqrt{GM/a_0}$ inextricably linking transport dynamics to the observed Baryonic Tully-Fisher relation [7, 8].

1.3 Core dynamics and shell-theorem breakdown

A further consequence of the transport framework is the breakdown of the classical shell theorem in extended systems. Because the contribution of a mass element depends on its propagation distance, contributions from different parts of a system are no longer equivalent. Elements located farther away have experienced greater drift reduction and therefore contribute more strongly to the effective field. This asymmetry leads naturally to restoring forces in galactic cores and explains the observed stiff-core rotation behavior.

1.4 Scope of the present work

The goal of this paper is to develop a minimal, flux-conserving description of gravitational transport and to demonstrate how galactic-scale phenomena arise from this framework.

The analysis focuses on:

- The derivation of a unified analytical force law based on a rigorous, flux-conserving transport.
- The fundamental distinction between coherent baryonic interaction and statistical vacuum self-interaction.
- The mathematical proof that this transport geometry natively derives flat rotation curves and the empirical Baryonic Tully-Fisher relation.
- The geometric origin of stiff-core dynamics via the breakdown of the classical shell theorem.
- The establishment of a rigidly constrained, single-parameter master equation (Eq. 2.23) that makes the framework strictly falsifiable against high-precision galactic kinematic data, while eliminating the arbitrary curve-fitting associated with dark matter halo profiles.

Possible extensions of the model, including the behavior at very large radii and the role of microscopic interactions, are discussed but not developed in detail.

2. Theoretical Framework: Gravity as Transport with Progressive Redistribution

We treat gravitation as a directed transport of gravitational influence generated by baryonic mass and propagating through a vacuum medium capable of elastic self-interaction. The central assumption is that total gravitational transport is conserved, while its directional coherence is progressively redistributed through interactions with the vacuum. The constant, continuous feed of gravity from source masses – without time restrictions – is a requirement.

In this framework, the strength of the gravitational field is determined by the **local density of transported gravitational influence**. Since the total transport is conserved, any reduction in the effective outward drift velocity leads to an increase in transport density and therefore to an enhancement of the gravitational field $\propto r$ while the field geometrically falls off $\propto 1/r^2$. Effectively, such enhanced gravity will fall off only $\propto 1/r$. The emergence of deviations from Newtonian gravity is not associated with a qualitative transition to a different force, but with a **gradual buildup of transport density caused by progressive slowing of the effective transport velocity**.

2.1 Radial Transport and Geometric Baseline

In the absence of redistribution, gravitational transport propagates radially and produces the familiar inverse-square field

$$g_N(r) = \frac{GM}{r^2}. \tag{2.1}$$

M is the source mass. This follows from conservation of total transport in spherical symmetry,

$$4\pi r^2 J_N(r) = \Phi = \text{constant}, \tag{2.2}$$

where $J_N(r)$is the radial transport density for Newtonian gravity

2.2 Redistribution through Interaction

As gravitational transport propagates outward, it undergoes elastic interactions with the vacuum medium. At each interaction, the transport of gravity is shared among a growing number of force carriers while preserving its total magnitude. The directional component is therefore reduced per carrier but preserved in sum. These elastic interactions redistribute their directional coherence and thereby alter gravitational strength. This macroscopic transition—from a highly directed, coherent radial flux into a progressively shared, diffuse transport field—is consistent with the fundamental conservation principles of radiative transfer in a scattering medium [9]. When drift velocity decreases, the effective gravitational field becomes less coherent than the corresponding radial field.

The transport is progressively shared among an increasing number of vacuum participants. A constant source mass feeds continuously a constant flux into space, and the scattered force can use the time it takes to build a higher density. This leads to two simultaneous effects:

1. The number of carriers increases with distance
2. The effective outward drift velocity of gravity decreases

2.3 Fick's Law, Transport Sharing and Drift Velocity

In the conversion-dominated regime, we adopt an effective transport redistribution analogous to Fick's first law of diffusion [10], relating the radial gravitational flux to the gradient of the gravitational potential, without implying literal diffusive particle transport:

$$J_r = -D(r)\frac{d\Phi_g}{dr}, \tag{2.3}$$

where Φ_g is the gravitational potential and $D(r)$ is an effective transport coefficient. Substituting (2.6) into (2.5) yields

$$r^2 D(r)\frac{d\Phi_g}{dr} = \text{constant}. \tag{2.4}$$

If D were constant, this would imply $d\Phi_g/dr \propto 1/r^2$ and hence recover the Newtonian $1/r^2$ scaling. Thus, ordinary diffusion with constant transport properties does not by itself alter the force law. The modification arises when self-interaction causes the effective transport coefficient $D(r)$ to acquire a radial dependence through **progressive redistribution of directional coherence**.

As radial transport propagates and undergoes scattering, the directed force is progressively distributed among an increasing number of vacuum "participants". (we use the terminology of the analogue fluid-dynamic theory) The number of carriers sharing the conserved net force grows approximately proportional to the distance traveled:

$$N(r) \propto r/\lambda. \tag{2.5}$$

We assume only:

1. Scattering events are elastic and conserve total directed gravity.
2. Each scattering event redistributes a portion of the directed gravity among previously uncorrelated vacuum degrees of freedom.
3. The medium does not preferentially suppress or amplify transport; it only redistributes coherence.
4. The source of gravity is constantly feeding without time dependency.

Under these conditions, each collision increases the number of participants sharing the conserved radial flux. Since the total radial force flux is conserved even when scattered, the effective radial drift velocity $v_{\text{drift}}(r)$ decreases inversely with the number of participants:

$$v_{\text{drift}}(r) \propto \frac{1}{N(r)} \propto \frac{\lambda}{r}. \tag{2.6}$$

This scaling does not require detailed knowledge of microscopic structure; it follows directly from the existence of a constant mean transport path and a steady source. The effective diffusion coefficient from random free walk in 3 dimensions scales as

$$D(r) \propto \lambda v_{\text{drift}}(r). \tag{2.7}$$

Substituting (2.6) into (2.7) yields

$$\boxed{D(r) \propto \frac{\lambda^2}{r} \propto \frac{1}{r}.} \tag{2.8}$$

Thus, self-interaction naturally produces a radius-dependent transport coefficient.

2.4 Buildup of Transport Density

The gravitational field reflects the density of transported influence. Since transport is conserved, the density scales inversely with the product of drift velocity and area:

$$J(r) \propto \frac{1}{r^2\, v_{\text{drift}}(r)}. \tag{2.9}$$

Substituting the scaling of v_{drift},

$$J(r) \propto \frac{1}{r^2} \cdot \frac{r}{\lambda} = \frac{1}{\lambda r}. \tag{2.10}$$

This is the key result:

$$\boxed{\text{redistributed contribution} \propto \frac{1}{\lambda r}} \tag{2.11}$$

Thus, the $1/r$ behavior emerges directly from transport conservation and drift slowing, without invoking a separate force law.

2.5 The Statistical Nature of Vacuum Scattering

To quantify the gradual onset of transport redistribution, we must track the propagation history of the gravitational flux. In accordance with standard kinetic theory for mean free paths [11], the stochastic scattering of coherent radial gravity into a redistributed transport phase is best modeled by a Poisson distribution.

Since each scattering event shares the transported impulse among additional carriers, the cumulative reduction in drift velocity is proportional to the number of interactions k, and the corresponding density enhancement therefore scales linearly with k.

Let the dimensionless variable $x = r/\lambda$ represent the expected mean number of scattering interactions a given transport element has experienced after propagating a distance r.

The fraction of the original gravitational transport that has undergone exactly k scattering events is given by the standard Poisson probability mass function:

$$P_k(x) = \frac{x^k e^{-x}}{k!}. \tag{2.12}$$

This allows us to strictly compartmentalize the total conserved transport into distinct "generations" of scattering:

- **The Unscattered Generation** $(\boldsymbol{k = 0})$: $\boldsymbol{P_0(x) = e^{-x}}$. This represents the fraction of transport that has survived completely intact without hitting the vacuum scattering threshold.
- **The Scattered Generations** $\boldsymbol{k \geq 1}$): $\boldsymbol{P_1(x) = xe^{-x}}$, $\boldsymbol{P_2(x) = \frac{x}{2}e^{-x}}$, etc. These represent transport that has been shared among vacuum carriers once, twice, or multiple times.

Crucially, because $\sum_{k=0}^{\infty} P_k(x) = 1$, absolute flux conservation is rigorously maintained at every distance r. No gravitational influence is lost; it is simply redistributed across scattering generations.

2.6 Density Weights and the Drift Velocity of Generations

While the total *flux* is conserved across generations, the observable *gravitational field* depends on the local transport *density*. As established in Section 2.4, density scales inversely with drift velocity.

Each successive scattering event shares the outward directional impulse among an increasing number of vacuum carriers, incrementally reducing the effective drift velocity. Therefore, the transport density of a specific generation $\boldsymbol{k}$ is weighted by the number of times it has scattered. Following the momentum conservation principles of macroscopic fluid entrainment [12], each successive interaction sweeps new vacuum participants into the continuous shared transport pool, incrementally reducing the effective drift velocity of that generation.

- The unscattered flux ($\boldsymbol{k = 0}$) maintains the maximum drift velocity (the speed of light), and thus carries a baseline density weight of 1.
- The scattered flux ($k \geq 1$) experiences a proportional slowdown. The density enhancement weight for the $k - th$ generation scales directly with $\boldsymbol{k}$, representing the cumulative slowdown of transport carriers.

2.7 Derivation of the Exact Master Equation

To find the total observable gravitational field relative to the full classical Newtonian baseline (g/g_N), we sum the transport density contributions from all scattering generations from $k = 0$ to $k = \infty$:

$$\frac{g(r)}{g_N(r)} = P_0(x) + \sum_{\mathrm{k}=1}^{\infty} P_{\mathrm{k}}(x) \times k\,. \tag{2.13}$$

Substituting the Poisson probability function into the sum:

$$\frac{g(r)}{g_N(r)} = e^{-x} + \sum_{\mathrm{k}=1}^{\infty} \frac{k(x^k e^{-x})}{k!} \tag{2.14}$$

In probability theory, the infinite sum $\sum_{\mathrm{k}=0}^{\infty} kP_{\mathrm{k}}(x)$ defines the exact expected value (the mean) of the Poisson distribution, which is simply x. Because the $k = 0$ term contributes nothing to this particular sum ($0 \times P(0) = 0$), the entire scattered summation resolves elegantly to exactly x.

Thus, the infinite series of scattering generations collapses into a rigorous, exact analytical expression:

$$\frac{g(r)}{g_N(r)} = e^{-x} + x \tag{2.15}$$

Substituting $x = r/\lambda$ and $g_N(r) = GM_b/r^2$, we arrive at the **exact analytical expression for the gravitational field (our master equation)**:

$$\boxed{g(r) = \frac{GM_b}{r^2} e^{-r/\lambda} + \frac{GM_b}{\lambda r}} \tag{2.16}$$

By calculating the transition through the exact Poisson summation, the derivation guarantees a strictly monotonic buildup of gravitational strength without introducing arbitrary algebraic closures. The universe smoothly and completely converts coherent geometric gravity into a macroscopic fluid-dynamic transport.

2.8 The Dual Interaction Regimes and the Effective Source ($\sqrt{M_b}$)

As gravitational transport propagates outward, it is subject to two fundamentally distinct types of interaction, governed by the nature of the target cross-section.

i. Baryonic Interaction: When gravitational transport—whether radial or redistributed—encounters other baryonic matter (such as a planet or star), it interacts with a highly correlated, macroscopic structure. Let N denote the number of transport carriers associated with the source, which scales with baryonic mass $N \propto M_b$. Because this

structure acts as a deterministic, condensed cross-section, the interaction integrates the full classical intensity of the N carriers of the source field. Thus, gravitational interactions with baryonic mass (m) scale with the total baryonic source mass (M_b).

$$M_{\text{eff}}^{(\text{bar m})} \propto N \propto M_b. \tag{2.17}$$

$$g(r) \propto N \propto M_b. \tag{2.18}$$

ii. Vacuum Self-Interaction: When the transport—whether radial or redistributed—propagates through empty interstellar space, it does not encounter the macroscopic cross-section of baryonic matter but interacts with vacuum which is a random medium possessing no condensed macroscopic target. In scattering theory, when a field interacts with its own underlying medium rather than a structured target, the effective interaction cross-section is restricted to the statistical fluctuation of the field. For uncorrelated contributions, the effective coupling strength scales with the root-mean-square of the number of contributors, $\sqrt{N}$, rather than their sum N [9, 11]. The number of transport quanta N is still proportional to the source mass M_b, while the effective self-interaction of the vacuum-coupled transport scales as:

$$M_{\text{eff}}^{(\text{vac})} \propto \sqrt{M_b} \propto \sqrt{N}. \tag{2.19}$$

After successive conversions the reduced drift velocity builds extra gravity over distance relative to Newtonian gravity, and self-interaction scales $\propto \sqrt{M_b}$. But when, at a certain point the enhanced gravity encounters baryonic mass, the redistributed gravity acts just like radial coherent gravity to a test mass m – with the full force corresponding to $g(r)$ at that position, $F = mg$. The distinction between buildup via self-interaction $\propto \sqrt{M_b}$ and distributed transport versus the action of gravity when it encounters baryonic matter is essential.

2.9 The Macroscopic Transport Scale (λ)

This profound difference in interaction cross-sections dictates the macroscopic transition boundary of the galaxy. The universal vacuum medium provides a constant baseline kinematic scattering threshold, most easily estimated using the universal acceleration metric a_0.

λ is defined as the characteristic length scale governing the decay of coherent transport and the emergence of redistribution, and is related to the vacuum threshold through:

$$\frac{GM_b}{\lambda^2} = a_0. \tag{2.20}$$

Solving for λ yields the system-dependent transition length:

$$\lambda = \sqrt{\frac{GM_b}{a_0}}. \tag{2.21}$$

This reveals that λ is not an arbitrary constant, but the dynamic kinematic boundary arising directly from the interplay between the full baryonic cross-section (M_b) and the vacuum scattering limit (a_0).

To find the deep halo field, we take the fully redistributed asymptotic term from our master force equation (2.16), which is $g_{\mathrm{halo}}(r) \propto \frac{\mathrm{GM_b}}{\lambda r}$, and substitute the transition scale eq. (2.21):

$$g_{halo} \approx \frac{GM_b}{r(\sqrt{GM_b/a_0}} = \frac{\sqrt{GM_b a_0}}{r}. \tag{2.22}$$

Substituting this native self-interaction amplitude back into our master equation (2.16) yields a unified master force law for the gravitational field in terms of a_0 for $\lambda = \sqrt{GM_b/a_0}$:

$$\boxed{g(r) = \frac{GM_b}{r^2} e^{-r/\lambda} + \frac{\sqrt{GM_b a_0}}{r}.} \tag{2.23}$$

While practical numerical evaluations often retain the parameter λ for simplicity, equation (2.23) formally represents the kinematic unification of classical baryonic intensity and redistributed transport from vacuum self-interaction. The coherent inverse-square component decays exponentially, while the redistributed transport establishes a persistent $1/r$ contribution. This unified force law serves as the mathematical foundation for macroscopic galactic kinematics, the observable consequences of which—including flat rotation curves and empirical scaling laws—are explored in Section 3, while stiff core rotation is treated in section 4.

2.10 The Gravitation Potential at the Transition from Solar to Interstellar Space.

The gravitational acceleration represents the spatial gradient of the underlying scalar field ($g(r) = -d\Phi/dr$). Based on our total gravitational force eq. (2.16), we can derive the according unified gravitational potential by integrating the force equation: $\int g(r)dr$:

$$\Phi_{total}(r) = -\int \left[\frac{GM_b}{r^2} e^{-r/\lambda} + \frac{GM_b}{\lambda r}\right] dr \tag{2.24}$$

Integrating this expression yields the according analytical potential for the gravitationally coupled vacuum:

$$\Phi_{total}(r) = -\frac{GM_b}{r} e^{-r/\lambda} - \frac{GM_b}{\lambda} Ei\left(-\frac{r}{\lambda}\right) - \frac{GM_b}{\lambda} \ln\left(\frac{r}{\lambda}\right) \tag{2.25}$$

where $Ei(x)$ is the Exponential Integral. This unified potential seamlessly bridges the macroscopic boundaries. At short ranges ($r \ll \lambda$), the exponential decay $e^{-r/\lambda} \approx 1$, and the potential is heavily dominated by the strictly classical Newtonian term ($-GM_b/r$).

However, at deep galactic radii ($r \gg \lambda$), the unscattered geometric baseline physically decays, and the potential becomes strictly dominated by the logarithmic term ($-\frac{GM_b}{\lambda}\ln\left(\frac{r}{\lambda}\right)$). This is mathematically highly significant, as a logarithmic scalar potential is exactly the required geometry to natively sustain flat halo rotation curves without invoking extended dark matter density profiles.

3. Transition Behavior and Observational Regimes

The force law derived in Section 2 describes a continuous transition from a geometry-dominated regime to a redistribution-dominated regime. This transition is governed by the gradual buildup of transport density resulting from decreasing drift velocity.

3.1 Relative enhancement and relative conversion

The relative enhancement of total gravity g relative to the classical Newtonian baseline g_N emerges directly from the Poisson summation:

$$\frac{g(r)}{g_N(r)} = e^{-r/\lambda} + \frac{r}{\lambda} \tag{3.1}$$

The only parameter in this expression is the transport scale λ, and the relative enhancement depends entirely on the dimensionless distance r/λ. Because the unscattered coherent baseline decays while the scattered transport density builds linearly, the transition is smooth and strictly monotonic.

- At $r = \lambda$, the enhancement is $\frac{g}{g_N} \approx 0.37 + 1 = 1.37$
- At $r = 3\lambda$, the enhancement reaches $\frac{g}{g_N} \approx 0.05 + 3 = 3.05$

A critical measure of this transition is the total gravity relative to the *surviving* coherent Newtonian force (the unscattered flux). Dividing the total field by the surviving baseline yields:

$$\frac{g(r)}{g_N(r)e^{-r/\lambda}} = 1 + \frac{r}{\lambda}e^{r/\lambda} \tag{3.2}$$

- At $r = \lambda$, this ratio is approximately **3.72**, meaning the field is already overwhelmingly dominated by converted, redistributed transport.
- At $r = 3\lambda$, this ratio explodes to approximately **61.2**, demonstrating that virtually all observable gravity in the deep halo arises from scattered transport.

This confirms that the conversion of the baseline precedes the massive buildup of absolute force, leading to a gradual, native enhancement of the field controlled entirely by the distance traveled.

3.2 Solar System Regime: Local Radial Coherence

Within planetary systems, characteristic orbital distances satisfy $r \ll \lambda$. The survival fraction of coherent radial gravity remains extremely close to unity:

$$e^{-r/\lambda} \approx 1 \tag{3.3}$$

Simultaneously, the redistributed transport term (r/λ) is vanishingly small. Thus, the gravitational field around stars consists almost entirely of unscattered radial gravity:

$$g(r) \approx \frac{GM_b}{r^2} \tag{3.4}$$

At these scales, the redistribution is negligible because the distance is insufficient to cause meaningful drift velocity reduction. This mathematically guarantees the local preservation of Newtonian gravity and General Relativity [13, 14] within solar systems.

Importantly:

- The entire solar system free-falls within the galactic gravitational field.
- By the equivalence principle, uniform external fields do not alter internal orbital dynamics to first order.
- No deviation from general relativity due to measurable conversion within the solar system is expected.

Everywhere in the galaxy, masses create their own Newtonian “bubbles”, where the metric dominates and the internal motion is protected from the galactic acceleration regime by the equivalence principle for free falling bodies.

3.3 Redistribution-dominated regime

For $r \gg \lambda$,

$$g(r) \approx \frac{GM}{\lambda r}. \tag{3.5}$$

This behavior arises from the combined effect of:

- greatly enhanced transport force relative to Newtonian gravity
- reduced drift velocity while a constant source feeds gravity continuously
- geometric spreading through scattering and shared gravity

3.4 Origin of flat rotation curves and the Tully-Fisher relation

On galactic scales well outside the bulge ($r \gg \lambda$), the effective field is dominated by the redistributed vacuum self-interaction. As derived in Section 2.9, the dual interaction cross-sections dictate that this deep-halo field takes the native form:

$$g_{halo}(r) \approx \frac{\sqrt{GM_b a_0}}{r}. \tag{3.6}$$

Equating this redistributed field to the centripetal acceleration (V^2/r) yields:

$$\frac{V^2}{r} = \frac{\sqrt{GM_b a_0}}{r} \Rightarrow V^2 = \sqrt{GM_b a_0}. \tag{3.7}$$

Squaring both sides cleanly recovers the empirical baryonic Tully-Fisher relation [7, 8]:

$$V_f^4 = GM_b a_0 \tag{3.8}$$

In this framework, the observed scaling does not arise from phenomenological curve-fitting or dark matter halos [15, 5], but natively from the statistical self-interaction cross-section ($\propto \sqrt{M_b}$) of the gravitational transport propagating through a vacuum governed by a_0.

4. Breakdown of the Shell Theorem and Dominance of Harmonic Cores

Having established that the interstellar medium operates as a fully dispersed $1/r$ environment, we now examine the profound kinematic consequences for interior mass distributions. In the classical Newtonian limit ($\propto 1/r^2$), the inverse-square law ensures exact geometric cancellation of forces inside a spherically symmetric shell, leading directly to Newton's shell theorem.

.

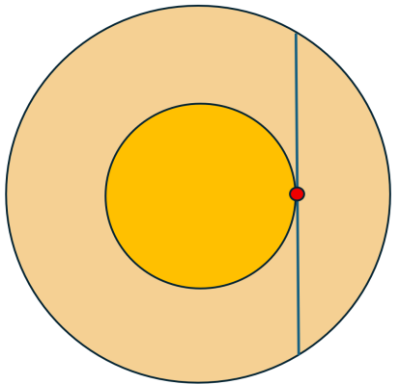

Figure 1 *shows a galactic core with assumed homogeneous mass distribution in each successive shell; inner radius R_1 and outer radius $R_2 = 2R_1$. A red test-mass is placed at*

R_1. Forces from the outside light orange donut exactly cancel out in Newton's shell theorem under the $1/r^2$ gravitational force. The net gravity on the test-mass comes from the mass inside R_1. Thus, gravity from masses outside R_1 left of the vertical chord cancels exactly with masses to the right when taken at the test-mass.

In the partly redistributed $1/r$ regime at the galactic interior, this geometric cancellation fundamentally fails, giving rise to unique core dynamics.

4.1 Double-Cone Derivation for a Giant Galaxy; the Breakdown of the Shell Theorem

In the Newtonian limit, the inverse-square law ensures exact cancellation of forces inside a spherically symmetric shell. This property follows directly from the $1/r^2$ geometry and leads to Newton's shell theorem.

Let us first consider a galaxy so large that the internal distances in the core allow us to treat it like a substantial part of gravity is converted to a $1/r$ transport regime. Then, consider a star displaced by x from the center of a spherical mass distribution of radius R. Take a narrow double cone of solid angle $d\Omega$ passing through the star, intersecting the shell at:

- Near patch A at distance $r_A = R - x$,
- Far patch B at distance $r_B = R + x$.

Mass element in each patch:

$$dm = \sigma r^2 d\Omega. \tag{4.1}$$

Under the effective transport kernel scaling $\propto 1/r$,

- Near-side force: $dF_A \propto \sigma r_A$.
- Far-side force: $dF_B \propto \sigma r_B$.

Net force contribution:

$$dF_{\text{net}} \propto (r_B - r_A). \tag{4.2}$$

Geometrically, $r_B - r_A \propto x$, then the interior acceleration is linear in displacement in a fully converted regime:

$$F_{\text{net}} = -kx \tag{4.3}$$

Thus solid-body rotation arises as a direct geometric consequence if the converted transport kernel is strongly dominating and acting within a finite mass distribution.

4.2 Harmonic Core Potential

The resulting potential inside an ideal fully converted bulge region is

$$\Phi(r) \propto r^2. \tag{4.4}$$

This is the potential of a simple harmonic oscillator.

Within a harmonic oscillator potential, the galactic cores naturally exhibit velocities:

$$V(r) \propto r, \tag{4.5}$$

consistent with solid-body rotation observed in many galactic cores.

When Ω is determined by the surrounding converted mass distribution, the net interior acceleration is linear in displacement:

$$g_{\text{core}}(r) \approx \Omega^2 r, \tag{4.6}$$

Equating this to the centripetal acceleration gives the same stiff rotation curve:

$$\frac{V^2}{r} = \Omega^2 r \quad \Rightarrow \quad V(r) \propto r, \tag{4.7}$$

Thus solid-body rotation arises as a direct geometric consequence of the converted transport kernel acting within a finite mass distribution.

Although galactic bulges are not perfectly spherical, the harmonic restoring behavior arises from the geometry of the $1/r$ kernel and persists under moderate departures from spherical symmetry.

4.3 Role of drift velocity

From Section 2, the effective drift velocity scales approximately as

$$v_{\text{drift}}(r) \propto \frac{\lambda}{r}. \tag{4.8}$$

Thus, the transport density scales as

$$\frac{1}{r^2\, v_{\text{drift}}} \propto \frac{1}{\lambda r}. \tag{4.9}$$

This means that contributions with longer propagation distance are intrinsically weighted more strongly. The asymmetry arises because:

$$r_B > r_A \quad \Rightarrow \quad v_{\text{drift}}(r_B) < v_{\text{drift}}(r_A), \tag{4.10}$$

and therefore

$$g_B > g_A. \tag{4.11}$$

Even a modest displacement (on galactic scales) produces a systematic imbalance between the two sides and the effective gravity generated.

4.4 From Radial to Partially Redistributed Interaction

In the present framework, transport over longer paths contributes more strongly due to drift reduction. Strong transport redistribution corresponds to an effective $1/r$ transport kernel, for which the shell theorem no longer holds. However, it is important to emphasize that exact $1/r$ behavior is not required to break the cancellation. Any transport enhanced by a significant $1/r$ kernel introduces an asymmetry between near-side and far-side contributions.

Thus, the relevant question is not whether the field has reached a pure $1/r$ form, but whether redistribution is sufficiently developed over the characteristic scale of the system. We don't need full conversion from radial to converted regime to achieve dynamics of this kind. From figure 1 it is evident that gravity from masses to the left side of the chord has a longer path and thus a stronger conversion than the near masses to the right. This makes a huge difference even in semi-converted regimes.

4.5 Role of central masses

There is also another factor contributing to the restoring force; the conversion of gravity from central masses may become significant already inside the core.

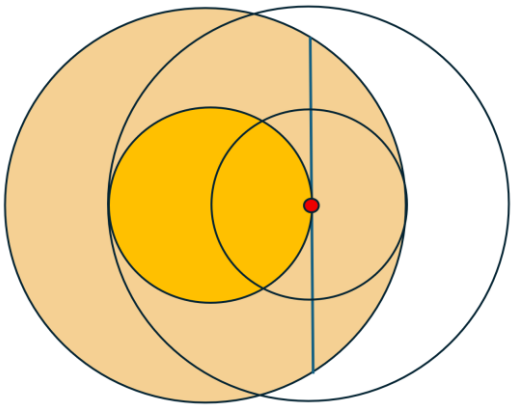

Figure 2 *demonstrates the propagation distances (concentric circles) from a specific test mass. The core is operating in a partly redistributed regime, the central mass interior to the test radius (the orange central mass) also pulls on the test mass with an amplified* $1/r$ *kernel rather than a purely classical* $1/r^2$ *kernel.*

As is evident from figure 2, in a partly converted $1/r$ regime, also the dark orange masses (inside the circle passing through our red spot) must contribute stronger gravity than the radial gravity would do. Again the masses at greater distance have more distance to convert gravity from radial to distributed transport. Hence there is a stronger and more restoring inward force coming from the masses inside the inner circle of the core as well. This serves as a compensating force for a possible shortcoming of the asymmetric $1/r$ contribution from the shell (the light orange donut) as analyzed in ch. 4.1.

The resulting interior force law depends on how strongly the kernel deviates from $1/r^2$over the size of the core.

- If redistribution is weak, the core remains close to Newtonian.
- If redistribution is strong across the entire core, the force approaches the harmonic form:

$$g(r) \propto r, \qquad V(r) \propto r. \tag{4.12}$$

- For intermediate cases (as expected when λ is comparable to the core diameter), the result is an approximately linear rise rather than an exact harmonic law. Contribution to the restoring force comes both from the extra inward force from distant masses in the shell and from extra inward force from distant masses inside the shell.

This provides a natural explanation for observed galactic cores:

- the inner rotation curves often rise nearly linearly,
- but are not perfectly harmonic,
- consistent with a partially redistributed interaction kernel.
- Larger galaxies are more converted and show more stiff solid-body rotation compared to dwarf galaxies

4.6 Onset of stiff-core behavior

For the Milky Way, adopting $\lambda \approx 5.8$ kpc, the inner few kiloparsecs correspond to $\mathrm{r}/\lambda \sim 0.5$.

For a mass at $r \approx 2.9$ kpc, the local field is only partially redistributed. However, contributions from the far side probe distances of order $r_B \sim 5.8$ kpc, corresponding to $r_B/\lambda \approx 1$.

Thus:

- near-side contributions remain only weakly redistributed,
- far-side contributions have undergone substantial redistribution,

leading to a rather strong asymmetry. Contributions from the far side have larger average propagation distances than those on the near side, contributing a more strongly enhanced force and reinforcing the imbalance. The asymmetry is sufficient to produce a restoring force.

4.7 Interpretation - Summary

The breakdown of the shell theorem in this framework is therefore not due to a change in the fundamental force law, but to the **distance dependence of transport history**. The transport framework naturally explains stiff-core rotation without requiring a fully developed $1/r$ field.

The essential mechanism is:

- transport is conserved, but redistributed
- drift velocity decreases with distance
- There is a constant, timeless feed from the source
- longer path → higher effective redistribution

As a result, distant mass elements contribute more strongly than nearby ones, breaking the exact cancellation of the shell theorem that holds for Newtonian gravity. This provides a purely geometric and transport-based explanation of core dynamics.

In standard Cold Dark Matter models, reproducing a solid-body core requires modifying the inner density profile to avoid the so-called cusp–core problem [16]. In the present framework, both regimes arise naturally from the geometry of the converted transport kernel.

5. Rotation Curves and Core–Halo Structure

The transport framework provides a unified interpretation of galactic rotation curves based on the redistribution of gravitational transport and the resulting buildup of transport density.

In this picture, different regions of a galaxy correspond to different regimes of transport history, rather than to different force laws. The same applies to different types of galaxies that may correspond to different regimes of transport history, not to different force laws.

5.1 The region between core and halo

Observed rotation curves typically exhibit:

- an inner core region with approximately linear velocity growth
- an outer halo region with nearly constant velocity

Between the inner and outer regions of a galaxy, the effective field is shaped by the complex spatial transition from the dense, harmonic geometry of the core (where partial

redistribution drives the breakdown of the shell theorem) to the fully mature, asymptotic $1/r$ self-interaction of the deep halo. In the transition region, there is a coexistence of:

- geometry-dominated contributions from core dynamics, $V \propto r$
- redistribution-enhanced contributions from halo dynamics, $V \propto const$
- radial Newtonian transport, $V \propto 1/\sqrt{r}$

This regime may be represented schematically as a superposition of contributions from core, halo, and residual inverse-square transport,

$$V^2(r) \approx a\,\Omega^2 r^2 + bK + c\frac{GM}{r}, \tag{5.1}$$

where the coefficients a, b, and c depend on position and mass distribution.

This expression captures the gradual transition between stiff-core behavior, halo behavior, and residual inverse-square transport. In the transition region, their coexistence can naturally lead to velocities exceeding the asymptotic halo value before flattening.

5.2 Dependence on galaxy size

The importance of redistribution depends on the ratio r/λ, where $\lambda = \sqrt{GM_b/a_0}$ and thus scale with the total mass of the galaxy

- **dwarf galaxies**
  The length of λ is critical, and sufficient redistribution depends on geometry and total baryonic mass. Partly stiff-body rotation of the core is expected because λ scales with total mass. Redistributed gravity is essential for halo rotation velocity to match their apparent "dark matter domination" [17].
- **Milky Way type galaxy**
  Sufficient redistributed transport breaks the shell theorem, giving approximately stiff-body rotation at the core. Redistributed gravity give ∝ constant halo rotation.
- **large spirals**
  The transport scale λ becomes large due to the system's baryonic mass. Extended core and transition region and clear stiff-body core structure, and an equally clear converted regime for the halo structure.

Thus, morphological diversity arises from the interplay between baryonic distribution and transport scale, rather than from variations in dark matter halos or in acceleration thresholds. The rotation curve is therefore a manifestation of the geometry of mass distribution and transport history across the system.

6. Atomic Physics, Spectral Invariance, and Lensing

The transport framework modifies the large-scale spatial distribution of gravitational influence while preserving local gravitational behavior. It is therefore important to clarify its implications for atomic physics and relativistic observables.

6.1 Local physics and spectral invariance

At small scales ($r \ll \lambda$), the gravitational field remains totally dominated by the inverse-square component.

Since the transport model:

- preserves the gravitational constant G,
- does not alter local spacetime structure,
- and does not modify quantum mechanics,

atomic transition energies and spectroscopic properties remain unchanged.

Even at galactic scales, the redistribution of transport modifies the spatial dependence of the field but does not introduce large potential differences over local systems. Thus, standard predictions for gravitational redshift remain valid within observational precision, where anomalies presently accounted for by adding dark matter is ascribed to the effect of transport enhanced baryonic gravity alone.

6.2 Gravitational lensing

In the weak-field limit, the effective potential governing motion and light propagation reflects the redistributed transport.

At large radii, the field approaches a $1/r$ form, corresponding to a logarithmic potential.

Because this contribution arises from accumulated transport rather than additional mass, the effective gravitational influence extends beyond that expected from baryonic matter alone.

This implies that light deflection on galactic scales can be enhanced relative to purely baryonic Newtonian predictions.

A full relativistic treatment would require embedding the transport law in a covariant metric description, which is beyond the scope of the present work.

6.3 Scope and limitations

The present framework describes a steady-state transport process in bound systems such as galaxies.

It does not attempt to address:

- the generation or propagation of gravitational waves
- strongly time-dependent or relativistic phenomena
- cosmological-scale evolution

These topics may require additional structure beyond the transport formulation developed here.

7. Conclusion

We have developed a transport-based framework for gravitation in which gravitational influence is described as a conserved outward transport that undergoes progressive redistribution through elastic interaction with the vacuum.

The present framework suggests that galactic-scale gravitational phenomena may be understood as consequences of transport dynamics rather than as evidence for additional unseen matter. The exact analytical force law derived in Section 2 provides a minimal macroscopic framework for this behavior, establishing the mechanism through which transport redistribution natively gives rise to observed galactic dynamics, eq. (2.16):

$$g(r) = \frac{GM}{r^2} e^{-r/\lambda} + \frac{GM}{\lambda r}.$$

7.1 Unified interpretation of gravitational regimes

Within this framework, different observed regimes of gravitational behavior arise from the same underlying transport mechanism:

- **Solar systems ($r \ll \lambda$)**
  Transport remains coherent and geometry-dominated, and the field reduces to the Newtonian form.
- **Transition region ($r \leq \lambda$)**
  In galactic cores redistribution becomes significant, and the field reflects a mixture of contributions with different propagation histories.
- **Galactic halos ($r > \lambda$)**
  The cumulative effect of reduced drift velocity produces an effective $1/r$ behavior, yielding flat rotation curves.

Thus, the observed large-scale deviations from Newtonian gravity emerge from transport dynamics rather than from modifications of the gravitational interaction or the introduction of additional matter components.

7.2 Core dynamics and shell-theorem breakdown

A key result of the present work is that the breakdown of the shell theorem in galactic cores arises from **differences in transport history across the system**.

This asymmetry produces a restoring force proportional to displacement and naturally explains the observed stiff-core rotation curves.

Importantly, this mechanism does not require the field to reach its asymptotic $1/r$ form locally. It arises in a partially redistributed regime and is therefore consistent with the observed structure of galactic cores.

7.3 Determination of the transport scale

The characteristic transport scale λ can be estimated from galactic data. In the present framework, λ is related to the baryonic mass of the system and can be estimated using eq. (2.16) as in Appendix A2.

For a Milky Way baryonic mass, this relation yields eq. (A.3)

$$\lambda \sim 5.4 – 6.3 \text{ kpc},$$

consistent with the values inferred from outer rotation curves and eq. (A.6)

Applying an average value of $\lambda \sim 5.8$ kpc and eq. (2.21)

$$\lambda = \sqrt{\frac{GM_b}{a_0}},$$

we get an estimate for a_0, a universal acceleration scale, eq (A.6):

$$a_0 \sim 2.7 \times 10^{-10}\, m/s^2.$$

Thus, λ should be interpreted as a system-dependent transport length, while a_0 represents the underlying universal scale governing the transition between regimes. This relation provides a natural link between the transport framework and observed galactic scaling relations.

7.4 Nature of the redistribution process

The redistribution process described in Section 2 leads to the cumulative effects observed at galactic scales.

The Poisson description of scattering provides a natural interpretation of how redistribution develops with distance, while the buildup of the redistributed component reflects the cumulative effect of repeated interactions.

This framework does not require a fully developed redistributed transport to become significant. Instead, it relies on progressive redistribution and transport delay as the fundamental mechanism.

7.5 Scope and limitations

The present work adopts a steady-state transport description based on endless feeding from a constant source and thereby avoids explicit time dependence. Thus, the source is allowed to use more time to fill in distant shells.

At very large radii, the redistributed structure may not be fully established if the feeding of the system becomes inefficient due to the decreasing effective drift velocity. This may lead to a weakening of the far outer halo, but such effects lie beyond the minimal model developed here.

7.6 Summary

The transport framework presented here provides:

- a unified explanation of gravitational behavior across scales
- a natural mechanism for flat rotation curves
- a geometric explanation of stiff-core dynamics
- a consistent interpretation based on transport conservation and drift reduction

The model retains the local validity of Newtonian gravity and General Relativity, while accounting for large-scale galactic phenomena without invoking non-baryonic dark matter.

Appendix A — Determination of the Transport Scale and Consistency Across Galactic Scales

A1 Purpose

The transport framework introduces a universal acceleration a_0 governing the vacuum's ability to scatter coherent gravitational momentum. For any given galaxy, this scale determines a system-dependent transport length $\lambda = \sqrt{GM_b/a_0}$, at which redistribution becomes dominant - λ represents an effective transport scale associated with a given system.

A2 Outer-Disk Estimate Using the Full Transport Law

This chapter provides a numerical estimate of the Milky Way's specific transport scale (λ_{MW}) using rotation curve data. Because the exact Poisson-derived master equation dictates that the Newtonian baseline exponentially decays, we can see how the fully redistributed transport dominates the deep halo.

Using eq. (2.16)

$$g(r) = \frac{GM_b}{r^2}\, e^{-r/\lambda} + \frac{GM_b}{\lambda r},$$

the circular speed is

$$v^2(r) = r\, g(r) = \frac{GM_b}{r} e^{-r/\lambda} + \frac{GM_b}{\lambda}. \qquad (A.1)$$

At $r = 25$ kpc, we take

$$v(25\ \text{kpc}) \approx 220\ km\ s^{-1},$$

and enclosed baryonic masses in the range

$$M_b(< 25\ \text{kpc}) \sim (6.1\text{–}7.0) \times 10^{10} M_\odot.$$

The corresponding values of λ are then obtained by solving

$$v^2(25\ \text{kpc}) = \frac{GM_b}{25\ \text{kpc}} e^{-\frac{25\ \text{kpc}}{\lambda}} + \frac{GM_b}{\lambda}. \qquad (A.2)$$

This gives approximately for $M_b(< 25\ \text{kpc}) \approx 6.1 \times 10^{10} M_\odot$, which gives $\lambda \approx 5.4$ kpc

and for $M_b(< 25\ \text{kpc}) \approx 7.0 \times 10^{10} M_\odot$, which gives $\lambda \approx 6.3$ kpc

The estimated range under these assumptions is

$$\boxed{5.4\ \text{kpc} \lesssim \lambda \lesssim 6.3\ \text{kpc}.} \qquad (A.3)$$

For the numerical examples below, one may adopt the representative intermediate value eq. (A.4)

$$\boxed{\lambda = 5.8\ \text{kpc}.} \qquad (A.4)$$

A3 Determination of the Universal Vacuum Threshold (a_0)

In the transport framework, the macroscopic transition length λ is not a rigid universal distance, but scales dynamically with the active baryonic mass of the system. The true universal constant is the vacuum's intrinsic momentum-scattering threshold, a_0.

As established in Section 2.9, the macroscopic transport scale is defined as the radius where the field dilutes to parity with this vacuum threshold:

$$\lambda = \sqrt{GM_b/a_0}$$

Rearranging this equation allows us to isolate and calculate the universal vacuum constant using the Milky Way's specific parameters derived above:

$$a_0 = \frac{GM_b}{\lambda^2} \qquad (A.5)$$

Taking the intermediate baryonic mass estimate $M_b \approx 6.5 \times 10^{10} M_\odot \approx 1.29 \times 10^{41} kg$ the standard gravitational constant $G \approx 6.674 \times 10^{-11} m^3 kg^{-1} s^{-2}$, and our derived transport length $\lambda \approx 5.8$ kpc $\approx 1.79 \times 10^{20} m$, we evaluate the threshold:

$$a_0 = \frac{GM_b}{\lambda^2} = 2.7 \times 10^{-10} \frac{m}{s^2} \quad (A.6)$$

This purely analytical derivation—achieved completely natively from the exact Poisson scattering limit—yields a universal vacuum parameter that is squarely in the correct order of magnitude relative to empirical kinematic fits ($a_0 \approx 1.2 \times 10^{-10} m/s^2$). The parameter a_0 acts as the universal vacuum metric that defines the macroscopic conditions for the dynamic scattering length.

A4 Solar-Point Force from λ Estimate

At the solar radius $R \approx 8\ kpc$, the enhancement relative to the full baryonic Newtonian field follows the exact dimensionless scaling:

$$\frac{g(r)}{g_N(r)} = e^{-r/\lambda} + \frac{r}{\lambda}. \quad (A.7)$$

For the given $\lambda \approx 5.8\ kpc$ ($r/\lambda \approx 1.38$), we estimate the total galactic gravity at our sun to be approximately **1.63** times the classical purely baryonic Newtonian prediction. Because 8 kpc is larger than λ, the local environment is fundamentally in a transport-dominated regime, though the unscattered baseline ($e^{-\frac{r}{\lambda}} = 0{,}25$) still provides about a quarter of the classical baseline's original strength.

Thus, the solar radius lies in a mixed regime:

- Halo dynamics constitutes the largest contribution
- Radial gravity still gives a considerable contribution
- Spillover from stiff-core dynamics may also contribute significantly.

For these reasons, using the solar-point to estimate λ is more uncertain than using $r = 25\ kpc$ as the primary determination of λ.

A5 Interpretation of the Interaction Scale

The parameter λ should be interpreted as the fundamental scattering length governing the macroscopic decay of the coherent Newtonian baseline. By using $x = r/\lambda$, one obtains a strict dimensionless scaling.

Unlike models that apply abrupt cutoffs or arbitrary algebraic closures, the Poisson limit dictates that the classical geometry decays progressively via $e^{-\frac{r}{\lambda}}$. This ensures that $r = \lambda$ does not represent a sudden onset of new physics, but rather the characteristic scale where the purely scattered transport (r/λ) definitively overtakes the dying unscattered transport.

A6 Milky Way Numerical values of g/g_N at galactic scales using $\lambda = 5.8$ kpc

Table A1

r(kpc)	r/λ	$e^{-r/\lambda}$	g/g_N	$g/g_N e^{-r/\lambda}$
1	0.17	0.84	1.01	1.20
2	0.34	0.71	1.05	1.48
3	0.52	0.60	1.11	1.85
4	0.69	0.50	1.19	2.38
5	0.86	0.42	1.28	3.05
6	1,03	0.36	1.39	3,86
8	1.38	0.25	1.63	6.52

g_N is the Newtonian gravitational field produced by baryonic matter in the absence of redistribution.

g/g_N represents the total gravitational field relative to the classical Newtonian baseline.

$e^{-r/\lambda}$ represents the fraction of transport that has not undergone any interaction.

$g/g_N e^{-r/\lambda}$ represents the total gravitational field relative to the remaining coherent transport. This quantity provides a direct measure of the scale of redistribution, since it compares the total field to the portion of transport that has not experienced drift reduction.

Even when the total enhancement g/g_N is modest, the effective ratio relative to the surviving coherent transport can be substantial.

This final column provides a profound measure of redistribution. For example, at 8 kpc, the total field is not merely 1.63 times the classical expectation; it is **6.47 times stronger** than the actual surviving unscattered baseline at that location. This demonstrates how heavily deep-galactic kinematics rely on the progressive buildup of the redistributed transport density.

A7 Summary

The numerical estimates indicates that:

- λ lies in the range 5.4–6.3 kpc.
- Significant redistribution begins smoothly at $r < \lambda$, providing the steep transition gradient required for stiff-core harmonic dynamics.

- The solar neighborhood at 8 kpc lies in a mostly redistributed transport-dominated regime.
- The purely scattered transport term correctly and natively isolates the deep-halo velocity, yielding an a_0 in good agreement with empirical observations.

These results support a consistent picture in which gravitational behavior on galactic scales is governed by transport history and drift reduction with a continuous feed from the source.

Appendix B — Supporting Considerations and Extensions of the Transport Framework

B1 Purpose

This appendix summarizes supporting arguments and possible extensions of the transport framework. These considerations are not required for the derivation of the force law in Section 2 but provide additional physical insight into the robustness and limitations of the model.

B2 Origin of the $1/\lambda r$ spatial scaling

A central result of the macroscopic transport framework is the emergence of a redistributed geometric kernel scaling as eq. (2.10): Transport Density $\propto \frac{1}{\lambda r}$,

$$g(r) \propto \frac{1}{\lambda r}.$$

This follows directly from three assumptions:

- conservation of total transport,
- endless feeding of gravity from the source, no time dependency
- progressive sharing of transport among an increasing number of carriers,
- geometric spreading over spherical surfaces.

If the number of carriers grows approximately as eq. (2.5)

$$N(r) \propto \frac{r}{\lambda},$$

then the effective drift velocity scales as eq. (2.6)

$$v_{\text{drift}}(r) \propto \frac{1}{N(r)} \propto \frac{\lambda}{r}.$$

Since the transport density is inversely proportional to both area and drift velocity, eq. (2.9),

$$J(r) \propto \frac{1}{r^2\, v_{\text{drift}}(r)} \propto \frac{1}{\lambda r},$$

which directly yields the observed scaling.

This result is independent of the detailed microscopic mechanism, but determined by the system-dependent transport scale λ.

B3 Microscopic Coupling and the Macroscopic Transport Length

The parameter λ introduced in Section 2 represents the macroscopic transport scale over which the coherent radial gravity is effectively redistributed into the diffusive transport regime.

However, it is conceptually vital to distinguish between the microscopic properties of the vacuum and the macroscopic dynamics of the transport field. In a continuous entrainment framework, interaction with the vacuum is not necessarily a sequence of discrete, wide-angle collisions, but rather a continuous microscopic coupling or "drag" between the propagating field and the underlying medium.

We must therefore distinguish between:

- **The universal vacuum coupling threshold (a_0):** A fundamental, intrinsic property of the interstellar medium, independent of any celestial source.
- **The macroscopic transport scale (λ):** The integrated distance required for the continuous microscopic coupling to cumulatively reduce the effective drift velocity of the primary coherent stream by a factor of e.

Because a massive, highly coherent gravitational flow from a giant spiral galaxy possesses significantly more transport inertia (M_b), it requires a longer integration distance to be macroscopically redistributed than the weaker flow from a dwarf galaxy, even though both propagate through the exact same universal vacuum.

This natively explains why the effective macroscopic transition scale is mass-dependent $\lambda = \sqrt{GM_b/a_0}$, while the underlying vacuum medium remains strictly universal.

B4 Limitation of the far-field from finite feeding speed

The force law derived in Section 2 assumes that the redistributed gravitational field is fully established as a steady-state transport configuration. This assumption is well justified at inner and intermediate galactic scales.

However, the transport framework also implies that the effective outward drift velocity decreases as transport is shared among an increasing number of carriers, scaling as:

$$v_{drift}(r) \sim c\left(\frac{\lambda}{r}\right)$$

Because the transport velocity drops inversely with distance, the time required to establish the redistributed structure at a given radius from a source grows quadratically. Integrating the drift velocity yields an effective feeding time:

$$t(r) \sim \frac{r^2}{2c\lambda}$$

At sufficiently large radii, this feeding time becomes extremely long. For λ estimated at 5.8 kiloparsecs, the outermost shells correspond to effective transport times drastically longer than simple light-travel distances. In this regime, the assumption of a fully established steady-state configuration may break down for $r \gg \lambda$.

B5 Phenomenological representation

A convenient way to represent this effect is to introduce an attenuation factor $A(r)$ multiplying the redistributed term,

$$g(r) = \frac{GM}{r^2} e^{-r/\lambda} + \frac{GM}{\lambda r} A(r), \qquad (B.6)$$

where

$A(r) \approx 1$ for inner and intermediate galactic scales,
$A(r) < 1$ at very large radii.

The value of $A(r)$ drops with increasing radius. The present work does not attempt to determine the functional form of $A(r)$. The purpose of this discussion is to emphasize that the ideal steady-state $1/r$ behavior based on a constant feed in an unlimited time perspective together with and a growing need for feed by increasing radii may not extend indefinitely in a dynamic system like a galaxy in motion through vacuum.

Physical implications: This provides a natural mechanism for:

- a gradual decline of rotation velocities at large radii
- a finite extent of galactic gravitational influence according to the enhanced model
- the avoidance of an indefinitely extended logarithmic potential

These effects arise without modifying the fundamental transport mechanism of gravity.

References

[1] A. Einstein, Die Grundlage der allgemeinen Relativitätstheorie, Annalen der Physik 49, 769–822, 1916.

[2] V. Rubin and W. Ford, Rotation of the Andromeda Nebula from a Spectroscopic Survey of Emission Regions., The Astrophysical Journal, 159, 379, 1970.

[3] Y. Sofue and V. Rubin, Rotation Curves of Spiral Galaxies., Annual Review of Astronomy and Astrophysics, 39(1), 137-174, 2001.

[4] F. Zwicky, Die Rotverschiebung von extragalaktischen Nebeln., Helvetica Physica Acta, 6, 110–127., 1933.

[5] T. van Albada and R. Sancisi, Dark Matter in Spiral Galaxies., Philosophical Transactions of the Royal Society of London, 320, 447, 1986.

[6] M. Milgrom, A Modification of the Newtonian Dynamics as a Possible Alternative to the Hidden Mass Hypothesis., The Astrophysical Journal, 270, 365, 1983.

[7] R. Tully and J. Fischer, A New Method of Determining Distances to Galaxies., Astronomy and Astrophysics, 54, 661, 1977.

[8] S. McGaugh et al, The Baryonic Tully-Fisher Relation., The Astrophysical Journal Letters, 533, L99, 2000.

[9] S. Chandrasekhar, Radiative Transfer, Oxford University Press, 1950.

[10] S. Chandrasekhar, Stochastic Problems in Physics and Astronomy., Reviews of Modern Physics, 15(1), 1-89, 1943.

[11] F. Reif, Fundamentals of Statistical and Thermal Physics, McGraw-Hill, 1965.

[12] L. Landau and E. Lifshitz, Fluid Mechanics, Course of Theoretical Physics, Volume 6, Pergamon Press, 1959.

[13] C. Will, The Confrontation between General Relativity and Experiment., Living Reviews in Relativity, 17, 4, 2014.

[14] J. Williams, S. Turyshev and D. Boggs, Progress in Lunar Laser Ranging Tests of Relativistic Gravity., Physical Review Letters, 93, 261101., 2004.

[15] A.-C. Eilers et al, The Circular Velocity Curve of the Milky Way from 5 to 25 kpc with APOGEE and Gaia DR2., The Astrophysical Journal, 871, 120, 2019.

[16] B. Moore, Evidence against dissipationless dark matter from the rotation curve of the Milky Way., Nature, 370, 629, 1994.

[17] A. Klypin et al, Where Are the Missing Galactic Satellites?, The Astrophysical Journal, 522, 82, 1999.